Synthesis and Efficacy of Silver and Zinc Oxide Nanoparticles from *Xenorhabdus stockiae* PB09 Cell-free Supernatant for Controlling Mushroom Mites

Prapassorn Bussaman[1,*], Paweena Rattanasena[2], Araya Kontaku[1] and Nakarin Pangsrisan[1]

Abstract

Biological control of mushroom mite (*Luciaphorus perniciosus* Rack) by cell-free supernatant of *Xenorhabdus stockiae* PB09, a nematode-symbiotic bacterium, has been shown to be successful, and this needs further development into more effective formulations. Presently, nanotechnology plays an important role in the development of several biological control agents. In this study, cell-free supernatant of *Xenorhabdus stockiae* PB09 was synthesized into silver and zinc nanoparticles using $AgNO_3$ and $Zn(NO_3)_2$ as precursors and then examined for chemical and physical characteristics as well as biological control activity against *L. perniciosus* Rack. Both silver and zinc nanoparticles (AgNPs and ZnNPs, respectively) synthesized from *X. stockiae* PB09 cell-free supernatant were shown to form at 350 nm as revealed by UV-visible spectrophotometry. Fourier transform infrared spectroscopy (FTIR) analysis showed that the major functional groups of AgNPs and ZnNPs were amide and amine. Also, scanning electron micrographs (SEM) of AgNPs and ZnNPs illustrated that they have triangular and hexagonal crystals, and dynamic light scattering (DLS) analysis showed that most of the particles found in AgNPs and ZnNPs were small and had organized dispersion. The acaricidal efficacies of AgNPs and ZnNPs were found to be highest against *Luciaphorus perniciosus* Rack at the mortality rates of 93.33±3.33% and 83.33±5.06%, respectively, which were 21.11% and 11.11% higher than cell-free supernatant of *X. stockiae* PB09. Hence, AgNPs and ZnNPs synthesized from cell-free supernatant of *X. stockiae* PB09 cell-free supernatant could be beneficial in the future development of safe and effective biological control agents against mushroom mites.

Keywords: Silver nanoparticles, Zinc nanoparticles, Xenorhabdus, Acaricidal activity, *Luciaphorus perniciosus*

[1] Department of Biotechnology, Faculty of Technology, Mahasarakham University, Maha Sarakham 44150 Thailand

[2] Department of Applied Sciences, Faculty of Science and Technology, Phranakhon Si Ayutthaya Rajabhat University, Phranakhon Si Ayutthaya 13000 Thailand

* Corresponding author(s), e-mail: prapassorn.c@msu.ac.th

1. Introduction

The trend of controlling the insect pests has been changed in the recent years due to the hazardous and prolonged effects of chemical insecticides and pesticides. Hence, several entomopathogenic bacteria have been studied to be used as safe biological control agents. *Xenorhabdus* spp. are Gram-negative bacteria belonging to the family Enterobacteriaceae that were found to associate with entomopathogenic nematodes of the family Steinernematidae (Forst *et al*., 1997). These bacteria and their nematodes were found to have rather complicated cooperation which resulting in robust toxicity to many types of insects (Akhurst, 1983). Xenorhabdus bacteria were found to produce 3 major extracellular products, including toxin complexes, hydrolytic enzymes and secondary metabolites that having different effects on mushroom mites and other insect pests. Toxin complexes were toxic proteins that causing toxemia in insects and resulting in paralysis and suppression of biological activities, as well as destroying hormonal glands (Nielsen-Leroux *et al*., 2012). Hydrolytic enzymes, including chitinase, lipase, phospholipase and protease, were produced by both bacteria and their nematode hosts, and they could cause necrosis in insect's fat body and also induce the production of haemolysin which destroying insect's blood cells (Forst and Nealson, 1996). Lastly, the bacterial secondary metabolites, including xenocomacins, xenorhabdin and xenoxide, were found to play the important roles in inhibition of other surrounding bacteria that living inside the same insect's body (Bode, 2009). Cell suspensions and cell-free supernatants of *Xenorhabdus* spp. have been successfully used for controlling of several insect pests, for instance, *Plutella xylostella* L. (Abdel-Razek, 2003; Mahar *et al*., 2005), *Hopila philanthus* (Fuessly) (Ansari *et al.,* 2003) and mushroom mite *(Luciaphorus perniciosus* Rack) (Bussaman *et al*., 2009). Additionally, cell-free supernatant of *Xenorhabdus stockiae* PB09 has been shown to effectively control the mushroom mites at the mortality rate of 89% (Bussaman *et al*., 2009). Therefore, it is interesting to explore the application of *Xenorhabdus stockiae* PB09 cell-free supernatant in various formulations to enhance its efficacy in controlling the insect pests. In the recent years, silver (Ag) and zinc (Zn) nanoparticles have been widely applied to be used as antimicrobial agents. For example, silver nanoparticles generated from $AgNO_3$ and *Bacillus amyloliquefaciens* and *Bacillus subtilis* were shown to have antimicrobial activities against both Gram-negative and -positive bacteria, including *Escherichia coli, Pseudomonas aeruginosa, Salmonella* spp*., Staphylococcus aureus,* and *Streptococcus pyogenes* (Ghiuta *et al*., 2017). Silver nanoparticles synthesized from $AgNO_3$ and pomegranate (*Punica granatum*) peel extract were also applied for controlling of lepidopteran pest *Spodoptera litura* (Fab.) (Lepidoptera: Noctuidae) (Bharani and Namasivayam, 2017). Furthermore, zinc nanoparticles were used for inhibiting several postharvest fungal contaminants, including *Penicillium expansum, Alternaria*

alternata, Botrytis cinerea and *Rhizopus stolonifer* (Sardella *et.al*., 2017). Additionally, ZnO nanoparticles synthesized from *Momordica charantia* leaf extract were found to have acaricidal, pediculicidal and larvicidal activity against blood feeding parasites (Gandhi *et al*., 2017). Hence, in this study, cell-free supernatant of *X. stockiae* PB09 was synthesized into nanoparticles by using $AgNO_3$ and $Zn(NO_3)_2$ as precursors and evaluated for their efficacies against mushroom mites *(Luciaphorus perniciosus* Rack). The knowledge obtained from this study can be useful for future development of *X. stockiae* PB09 as safe and effective biological control agents.

2. Materials and Methods

2.1 Preparation of *Xenorhabdus stockiae* PB09 cell-free supernatant

By following the method of Bussaman *et al*. (2012), *X. stockia*e PB09 colonies were inoculated to tryptic soy broth (TSB) and incubated at 28±2°C and 200 rpm for 24 h. Then, *X. stockia*e PB09 culture was added to TSB at 10% v/v and incubated at 28±2°C and 200 rpm in the dark for 24, 48 and 72 h. The culture was then centrifuged at 10,000 rpm and 4°C for 20 min, and the derived supernatant was filtered through 0.22 µm-membrane and stored at 4°C for synthesis of nanoparticles. The experiment was performed in triplicates.

2.2 *Lentinus squarrosulus* (Mont.) Singer mushroom mycelium

According to the method of Bussaman *et al*. (2012), *L. squarrosulus* (Mont.) Singer mushroom mycelium was grown on a mixture of sterile sawdust and sorghum grain in glass bottle at 30±2°C for 1 week to establish a fresh spawn which was used for cultivating mushroom mites (*Luciaphorus perniciosus* Rack). *L. squarrosulus* (Mont.) Singer mycelium was also inoculated to potato dextrose agar (PDA) in Petri dish plates and incubated at 30±2°C until the mycelium was fully grown. After that, the mycelium was punctured by sterile 5-mm cork borer and the mycelial plugs were placed upside down on PDA in 5-cm Petri dish plate and incubated at 30±2°C until the mushroom mycelium fully grew to cover the surface of PDA which was then used for evaluating the acaricidal activity (activity against mushroom mites).

2.3 *Luciaphorus perniciosus* Rack mushroom mite

L. perniciosus Rack mites were kindly provided by Biological Control Research Unit at Mahasarakham University that isolated them from infested *L. squarrosulus* basidiocarps and composts obtained from Rapeephan mushroom farm in Khon Kaen province in the Northeast of Thailand. Both male and female mites were cultivated by using *L. squarrosulus* (Mont.) Singer mushroom mycelium that was grown on a mixture of sterile sawdust and sorghum grain in the glass bottle at 30±2°C (Bussaman *et al*., 2012).

2.4 Preparation of $AgNO_3$ nanoparticles (AgNPs) and $Zn(NO_3)_2$ nanoparticles (ZnNPs)

2.4.1 Preparation of $AgNO_3$ and $Zn(NO_3)_2$ aqueous solutions

$AgNO_3$ and $Zn(NO_3)_2$ aqueous solutions were prepared at the concentration of 1,000 ppm according to Barapatre *et al*. (2016). In brief, 25 mg of $AgNO_3$ (168.87 g/mol) was diluted with 25 ml of sterile deionized water in volumetric flask and filtered through 0.22 µm-membrane. $AgNO_3$ solution was then kept in 30 ml-vial and covered with aluminum foil at 4°C. Also, 39.27 mg of $Zn(NO_3)_2$•$6HO_2$ (297.47 g/mol) was mixed with 25 ml of sterile deionized water, then filtered and stored using the same process.

2.4.2 Synthesis of AgNPs and ZnNPs by using *X. stockiae* PB09 cell-free supernatant

Synthesis of AgNPs and ZnNPs by using *X. stockiae* PB09 cell-free supernatant was performed according to the modified method of Barapatre *et al*. (2016). Briefly, $AgNO_3$ and $Zn(NO_3)_2$ aqueous solutions at 1,000 ppm (from section 2.4.1) were separately mixed with *X. stockiae* PB09 cell-free supernatant to the final concentration of $AgNO_3$ and $Zn(NO_3)_2$ at 6, 8, 10 and 12 ppm in the volume of 100 ml. The mixtures were incubated at 27°C and 100 rpm in the dark and then analyzed for the characteristics of AgNPs and ZnNPs and their acaricidal activities.

2.5 Physical characteristics of AgNPs and ZnNPs synthesized using *X. stockiae* PB09 cell-free supernatant

2.5.1 UV-visible spectrophotometry

UV-visible spectrophotometer was used to monitor the reductions of Ag^+ and Zn^{2+} ions and formations of AgNPs and ZnNPs according to the method of Barapatre *et al*. (2016). One milliliter of each AgNPs and ZnNPs that was synthesized using *X. stockiae* PB09 cell-free supernatant was analyzed by UV-visible spectrophotometer (UV 160A, Shimadzu, Japan) at the wavelength of 200-700 nm every 24 h for 5 d.

2.5.2 Fourier transform infrared spectroscopy (FTIR)

FTIR was employed for the study of AgNPs' and ZnNPs' functional groups by following method of Barapatre *et al*. (2016). One hundred milliliters of either AgNPs or ZnNPs that was synthesized using *X. stockiae* PB09 cell-free supernatant were centrifuged at 10,000 rpm for 20 min and the supernatants were filtered through 0.22 µm-membrane. Aqueous solutions of $AgNO_3$ and $Zn(NO_3)_2$ were added to the supernatants of AgNPs and ZnNPs, respectively, at the final concentration of 8 ppm and the mixtures were incubated at 28±2°C and 200 rpm for 24 h. Finally, the mixtures were dried by using freeze dryer, mixed with KBr, ground into fine powders , and analyzed by Fourier Transform Infrared Spectroscopy (FT-IR) (Shimadzu,

Japan) at the frequency ranging from 400 to 4,000 cm^{-1} . For all spectra, the baseline corrections were carried out.

2.5.3 Dynamic light scattering (DLS) analysis

DLS was used for analysis of AgNPs' and ZnNPs' particle sizes by following the method of Barapatre *et al*. (2016). AgNPs and ZnNPs that were synthesized using *X. stockia*e PB09 cell-free supernatant (100 mL) were centrifuged at 10,000 rpm for 20 min, and their supernatants were filtered through 0.22 µm-membrane, added with $AgNO_3$ and $Zn(NO_3)_2$ solutions, respectively, at the concentration of 8 ppm, and finally incubated at 28±2°C and 200 rpm for 24 h. The samples were dried by freeze-dryer and ground into fine powder for analysis of particle size distribution and Zeta (ζ) potential measurement by DLS-LS230 (Beckman-Coulter, USA).

2.5.4 Scanning electron microscopy (SEM)

The surface characteristics of AgNPs and ZnNPs were examined by SEM according to Patra and Baek (2017). The powders of AgNPs and ZnNPs that were synthesized using *X. stockia*e PB09 cell-free supernatant were attached to carbon tape on the stubs and then sprayed with gold particles for 150 sec under vacuumed condition and analyzed by SEM (LEO-1450VP, Zeiss, USA) at 15 kV at 500x, 2000x, 5000x, and 10,000x.

2.6 Bioassays

2.6.1 Effect of $AgNO_3$ and $Zn(NO_3)_2$ nanoparticles on *L. squarrosulus* (Mont.) Singer mushroom mycelium

Effect of $AgNO_3$ and $Zn(NO_3)_2$ nanoparticles on *L. squarrosulus* (Mont.) Singer mushroom mycelium was evaluated by poisoned food technique (Fang *et al*., 2014). PDA (5 ml) was mixed with either $AgNO_3$ or $Zn(NO_3)_2$ aqueous solutions (at 1000 ppm, prepared according to the section 2.4.1) to the final concentrations of 6, 8, 10 and 12 ppm, and the mixtures were poured into each of the 5-ml Petri dish plates. After that, mushroom mycelium on a 0.5 mm-agar plug (prepared according to the section 2.2) was placed upside down onto each of the $AgNO_3$- and $Zn(NO_3)_2$- PDA plates and incubated at 28±2°C for 3 days. PDA mixed with Carbendazim (commercial fungicide at 1,000 ppm) was used as positive control group.

2.6.2 Efficacy of AgNPs and ZnNPs synthesized using *X. stockia*e PB09 cell-free supernatant for controlling mushroom mites

The efficacy of AgNPs and ZnNPs synthesized using *X. stockia*e PB09 for controlling of mushroom mites was evaluated according to Bussaman *et al*. (2009). AgNPs and ZnNPs synthesized using *X. stockia*e PB09 cell-free supernatant at the final concentration of 6, 8, 10 and 12 ppm in the volume of 500 µl were separately sprayed onto each PDA plate that having

mushroom mycelium grown all over the surface. After that, 30 of 1 day old-female mushroom mites were placed onto sprayed mushroom mycelium. All PDA plates were incubated at 28±2°C. Mite mortality was recorded every day for 5 days consecutively. The positive control group was PDA mixed with 0.05 mg/mL Propargite (commercial acaricide). The rate of mite mortality was calculated as following:

$$\%\text{mite mortality} = [(A-B) \times 100] / A$$

where A = number of dead mite(s) in the positive control group (being sprayed with Propargite) and B = number of dead mite(s) in the tested groups being sprayed with AgNPs and ZnNPs synthesized using *X. stockia*e PB09 cell-free supernatant.

2.7 Data analysis

The data were analyzed by using one-way analysis of variance (one-way ANOVA) and compared using Fisher's Least Significant Difference (LSD) test by SAS program (1990).

3. Results and Discussion

3.1 UV–visible spectroscopy of AgNPs and ZnNPs synthesized using *X. stockia*e PB09 cell-free supernatant

AgNPs and ZnNPs were preliminarily examined by UV–visible spectrophotometer to illustrate the surface plasma resonance (SPR) of the metal nanoparticles that could give the information of NP shape, size, and environment (Barapatre *et al*., 2016). In this study, AgNPs synthesized using *X. stockia*e PB09 cell-free supernatant was found to form at the wavelength of 320–450 nm with the maximum peak at 350 nm (Figure 1). The color of solution was transformed from light to darker shade which indicating the reduction of $AgNO_3$ and formation of AgNPs (Patra and Baek, 2017). Similarly, ZnNPs synthesized using *X. stockia*e PB09 cell-free supernatant was also found to form at the wavelength of 250-450 nm with the highest peak at 350 nm (Figure 2).

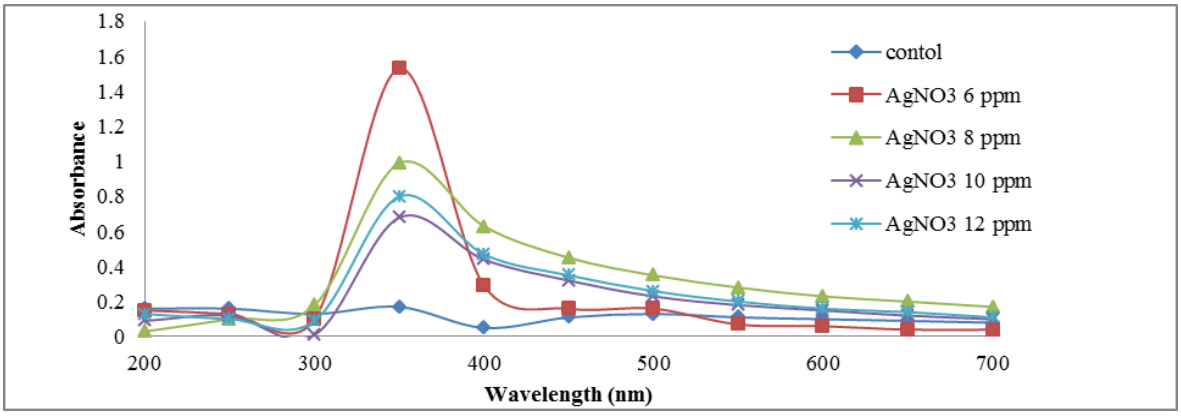

Figure 1 UV-visible spectra of AgNPs synthesized by using *X. stockia*e PB09 cell-free supernatant.

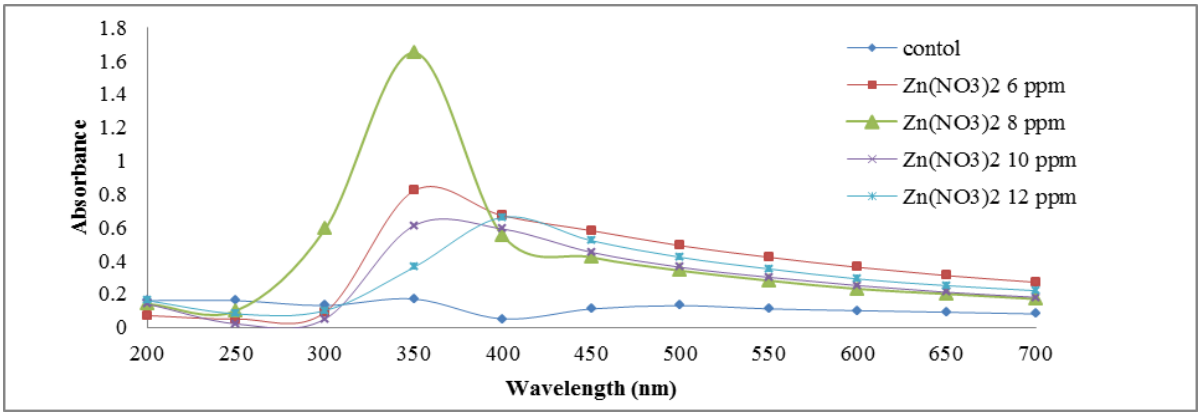

Figure 2 UV-visible spectra of ZnNPs synthesized by using *X. stockia*e PB09 cell-free supernatant

3.2 FTIR analysis of AgNPs and ZnNPs synthesized using *X. stockia*e PB09 cell-free supernatant

FTIR analysis was applied to evaluate the possible functionalities that may associate with metal reduction to metal nanoparticles (Ahmad *et al*., 2017). Figure 3–5 showed the FTIR spectra of *X. stockiae* PB09 cell-free supernatant, AgNPs- and ZnNPs synthesized using *X. stockia*e PB09 cell-free supernatant, respectively. *X. stockiae* PB09 cell-free supernatant was found to have the major bands at the wave number 3362 which may be from primary amide, 1647 and 1656 from secondary amide, and 1623, 1533 and 1557 from primary amine (Figure 3). Also, AgNPs synthesized using *X. stockia*e PB09 cell-free supernatant was shown to have peaks at 2909, 1647 and 1533 from primary amide, 1619 from secondary amide, and 1653 and 1509 from secondary amine (Figure 4). Similarly, ZnNPs synthesized using *X. stockia*e PB09 cell-free supernatant was found to have the major bands at the wave number 2909, 1647 and 1533 from primary amide, 1619 from secondary amide, and 1653 and 1509 from secondary amine (Figure 5). The results from FTIR analysis could be summarized in Table 1. Interestingly, ZnNPs synthesized using *X. stockia*e PB09 cell-free supernatant was found to have less changes of functional groups when compared to AgNPs synthesized using *X. stockia*e PB09 cell-free supernatant.

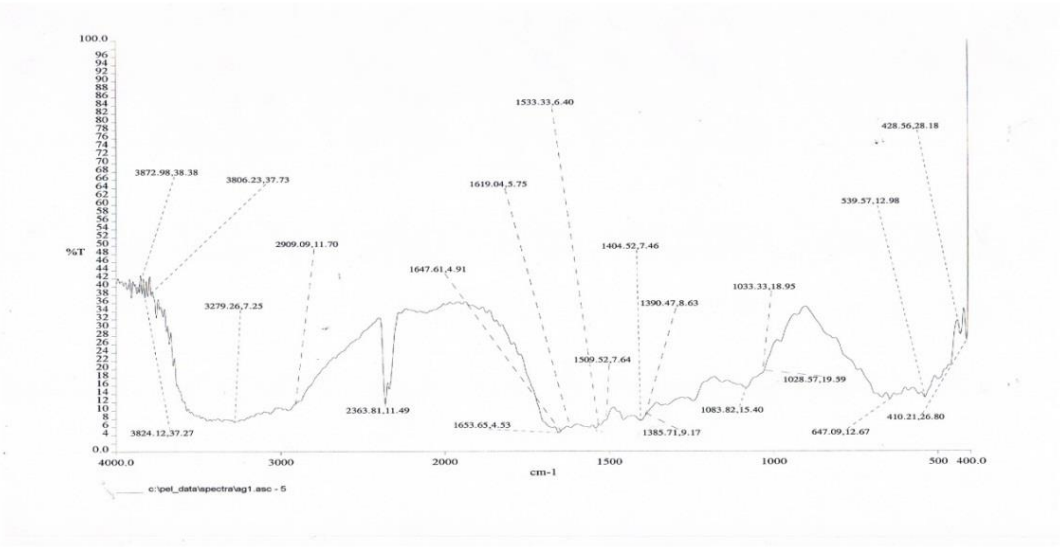

Figure 3 FTIR spectra of *X. stockiae* PB09 cell-free supernatant

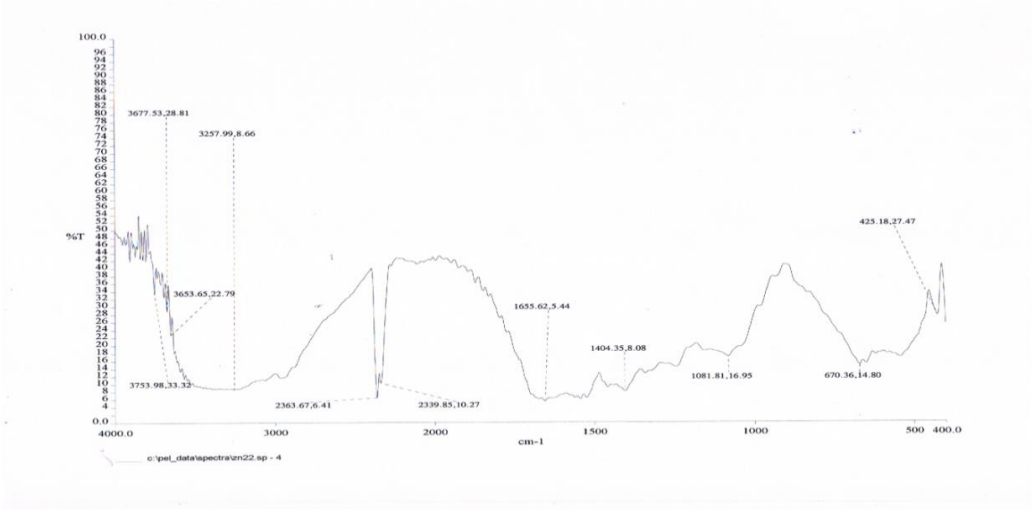

Figure 4 FTIR spectra of AgNPs synthesized using *X. stockia*e PB09 cell-free supernatant

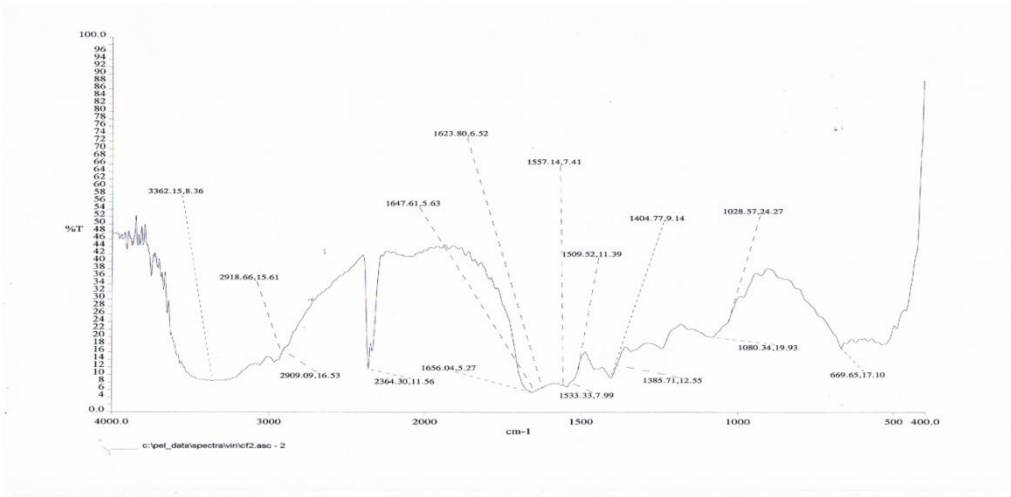

Figure 5 FTIR spectra of ZnNPs synthesized using *X. stockia*e PB09 cell-free supernatant

Table 1 Summary of FTIR analyzed-functional groups found in AgNPs and ZnNPs that were synthesized using *X. stockia*e PB09 cell-free supernatant

Compound	AgNPs	ZnNPs	Functional group
Amide I	+	+	N-H
Amide II	+	+	N-H
Amine I	-	+	N-H
Amine II	+	+	N-H
Alkane CH_2, CH_3	+	+	C-H
Aromatic	-	-	C=C
Ester	-	-	C-O
Chloride	+	+	C-Cl
Phenols	+	-	O-H
Ether and ester	+	+	C-O
Bromide	+	-	C-Br
Chloro-Iodide	+	+	C-I

3.3 Dynamic light scattering (DLS) analysis of AgNPs and ZnNPs synthesized using *X. stockia*e PB09

DLS was applied to illustrate the particle size and dispersion (Ahmad *et al*., 2017). Figure 6 revealed that *X. stockiae* PB09 cell-free supernatant had large particles which dispersing in disorganized pattern. It was also found to have the particles smaller than 10 µm only for 3.19% and smaller than 100 µm for 25.70%. In contrast, AgNPs synthesized using *X. stockia*e PB09 cell-free supernatant was shown to have small particles, of which sizes < 1 µm accounting for 1.23%, < 10 µm for 7.73%, < 100 µm for 34.30% and < 100 µm, and the size of the smallest particle was 0.782 µm (Figure 7). The particles of AgNPs synthesized using *X. stockia*e PB09 cell-free supernatant was also found to disperse in organized and uniformed pattern. In addition, the particles of ZnNPs synthesized using *X. stockia*e PB09 cell-free supernatant were found to disperse in both organized and disorganized patterns, with the sizes of < 1 µm accounting for 0.43%, < 10 µm for 6.37%, < 100 µm for 48.50%, and the smallest particle was 0.375 µm (Figure 8).

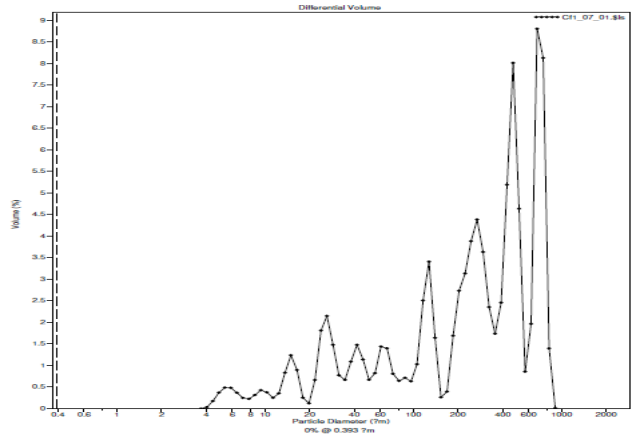

Figure 6 Size and dispersion of *X. stockiae* PB09 cell-free supernatant

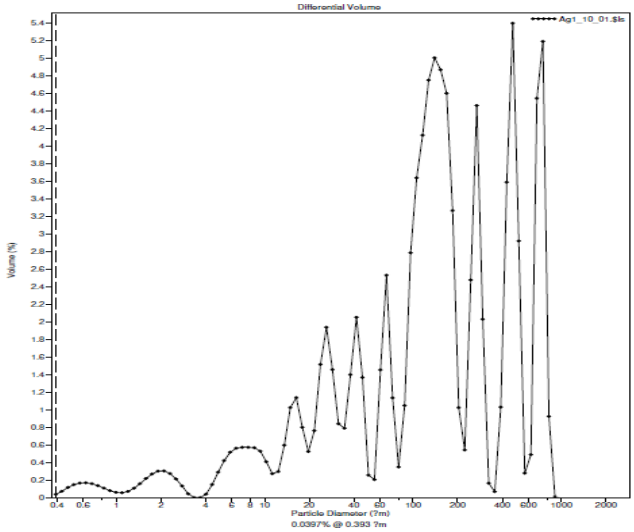

Figure 7 Size and dispersion of AgNPs synthesized using *X. stockiae* PB09 cell-free supernatant

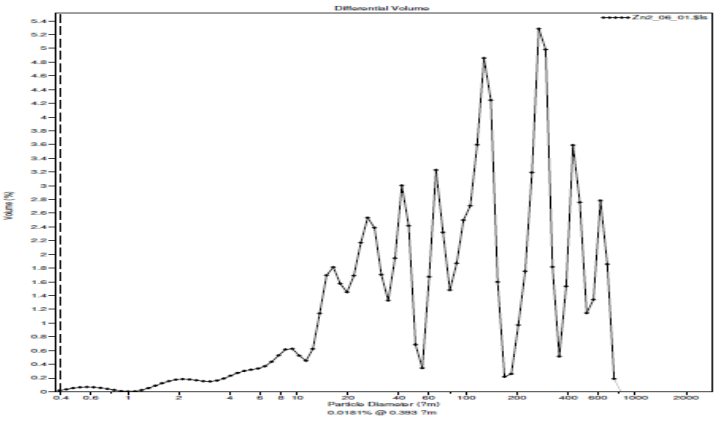

Figure 8 Size and dispersion of ZnNPs synthesized using *X. stockiae* PB09 cell-free supernatant

3.4 Scanning electron microscopy (SEM) analysis of AgNPs and ZnNPs synthesized using *X. stockiae* PB09 cell-free supernatant

Morphology and surface characteristics of nanoparticles can be observed through SEM technique (Ghiuta *et al*., 2017). Figure 9 showed that the morphology of cell-free supernatant of *X. stockiae* PB09 (Fig. 9A) was smoother than AgNPs and ZnNPs synthesized using *X. stockiae* PB09 cell-free supernatant (Figure 9B and C, respectively). The morphology of AgNPs was found to have triangular crystals (Figure 9B) that were smaller than the hexagonal crystals of ZnNPs synthesized using *X. stockiae* PB09 cell-free supernatant (Figure 9C).

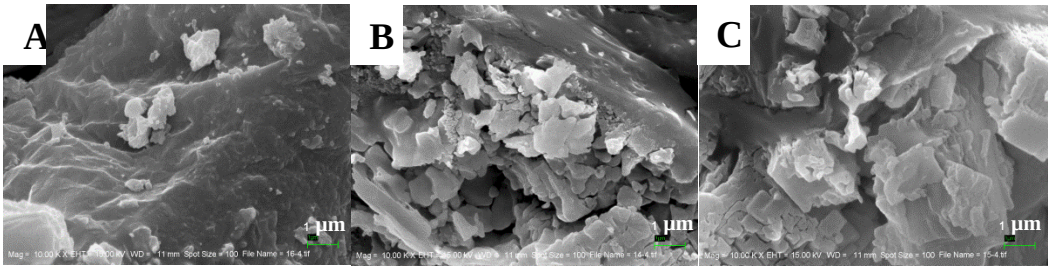

Figure 9 Scanning electron micrographs of (A) cell-free supernatant of *X. stockiae* PB09, (B) AgNPs, and (C) ZnNPs synthesized using *X. stockiae* PB09 cell-free supernatant at 10,000x magnification

3.5 Bioassay results

3.5.1 Effect of $AgNO_3$ and $Zn(NO_3)_2$ nanoparticles on *L. squarrosulus* (Mont.) Singer mushroom mycelium by poisoned food techniques

L. squarrosulus (Mont.) Singer mushroom mycelium was found to be capable of growing normally in the negative control PDA (Figure 10C) and also the PDA that were mixed with aqueous solutions of $AgNO_3$ (Figure 10A) and $Zn(NO_3)_2$ (Figure 10B) at the concentrations of 6, 8, 10, and 12 ppm. On the contrary, the positive control group that applying with fungicide Carbendazim (Figure 10D) showed no growth of mushroom mycelium. This may suggest that $AgNO_3$ and $Zn(NO_3)_2$ nanoparticles had no toxic or inhibitory effects on the growth of *L. squarrosulus* (Mont.) Singer mushroom mycelium.

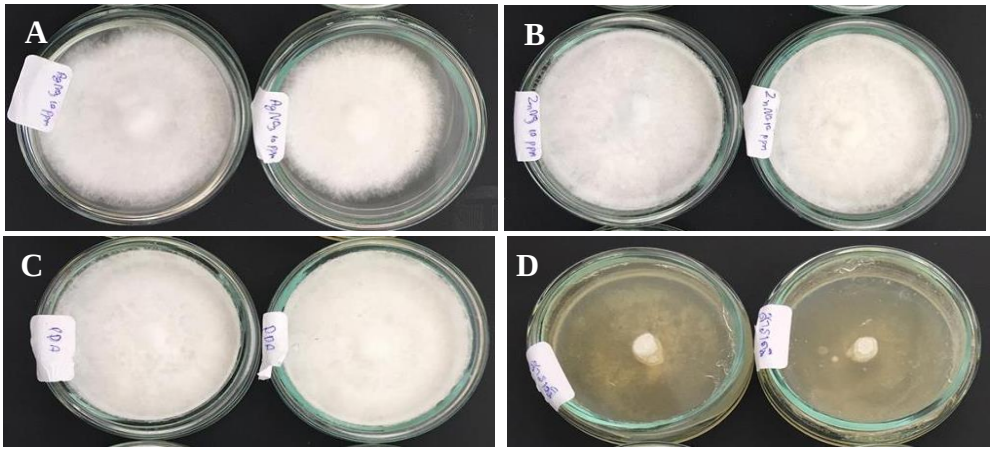

Figure 10 Growth of *L. squarrosulus* (Mont.) Singer mushroom mycelium on (A) PDA mixed $AgNO_3$ solution, (B) PDA mixed with $Zn(NO_3)_2$ solution, (C) negative control PDA and (D) positive control PDA mixed with fungicide Carbendazim

3.5.2 Acaricidal activities of AgNPs and ZnNPs synthesized using *X. stockia*e PB09 cell-free supernatant against mushroom mites

AgNPs synthesized using *X. stockia*e PB09 cell-free supernatant was evaluated against *Luciaphorus perniciosus* Rack mushroom mites and found to be up to 21.11% more effective than cell-free supernatant of *X. stockia*e PB09 in causing mite mortality (Table 2). The efficacy of AgNPs synthesized using *X. stockia*e PB09 cell-free supernatant was found to be highest at 72 h when this was applied at 8 ppm (93.33±3.33% mite mortality), followed by 10 ppm (88.89±5.09%mite mortality).

Furthermore, ZnNPs synthesized using *X. stockia*e PB09 cell-free supernatant was also found to be more effective than cell-free supernatant of *X. stockia*e PB09 by causing the mite mortality up to 11.11% higher (Table 3). The efficacy of ZnNPs synthesized using *X. stockia*e PB09 cell-free supernatant also reached its peak at 72 h and caused the maximum mite mortality when applying at 8 ppm (83.33±5.09% mite ,mortality), followed by 12 ppm (82.22±3.85%mite mortality); however, this was found to be moderately lower than that of AgNPs synthesized using *X. stockia*e PB09 cell-free supernatant.

Table 2 Acaricidal activities of AgNPs synthesized using *X. stockiae* PB09 cell-free supernatant at the different concentrations

Treatment	% Mite mortality			
	24 h	48 h	72h	96 h
Cell-free upernatant	63.33±3.33^{dA}	70.00±5.77^{dA}	72.22±5.09^{dA}	70.00±6.67^{cA}
AgNPs 6 ppm	68.89±6.94^{cdB}	71.11±6.94^{cdB}	85.56±3.85^{cA}	72.22±3.85^{bcB}
AgNPs 8 ppm	73.33±5.77^{bcC}	84.44±6.94^{bAB}	93.33±3.33^{abA}	77.78±1.92^{bBC}
AgNPs 10 ppm	74.44±5.09^{bcB}	80.00±5.77^{bcAB}	88.89±5.09^{bcA}	76.67±6.67^{bcB}
AgNPs 12 ppm	77.78±6.94^{bA}	77.78±5.09^{bcdA}	84.44±5.09^{cA}	78.89±5.09^{bA}
TSB	0.00±0.00^{eA}	0.00±0.00^{eA}	0.00±0.00^{eA}	0.00±0.00^{dA}
Propagite	100.00±0.00^{aA}	100.00±0.00^{aA}	100.00±0.00^{aA}	100.00±0.00^{aA}

Note: The data were presented as mean ± standard deviation. TSB = tryptic soy broth; Propargite = acaricide at 0.05 mg/ml; Means within the same column followed by the same lower case letters are not significantly different (p<0.05) as compared by LSD test; Means within the same row followed by the same upper case letters are not significantly different (p<0.05) as compared by LSD test.

Table 3 Acaricidal activities of ZnNPs synthesized using *X. stockiae* PB09 cell-free supernatant at the different concentrations

Treatment	% Mite mortality			
	24 h	48 h	72 h	96 h
Cell-free supernatant	63.33±3.33^{cA}	70.00±5.77^{cA}	72.22±5.09^{cA}	70.00±6.67^{cA}
ZnNPs 6 ppm	63.33±5.77^{cA}	72.22±1.92^{cA}	73.33±6.67^{cA}	68.89±8.39^{cA}
ZnNPs 8 ppm	71.11±5.09^{bB}	75.56±1.92^{bcB}	83.33±5.09^{bA}	74.44±1.92^{bcB}
ZnNPs 10 ppm	68.89±5.09^{bcA}	71.11±6.94^{cA}	77.78±5.09^{bcA}	74.44±5.09^{bcA}
ZnNPs 12 ppm	72.22±3.85^{bB}	82.22±3.85^{bA}	82.22±3.85^{bA}	82.22±6.94^{bA}
TSB	0.00±0.00^{dA}	0.00±0.00^{dA}	0.00±0.00^{dA}	0.00±0.00^{dA}
Propagite	100.00±0.00^{aA}	100.00±0.00^{aA}	100.00±0.00^{aA}	100.00±0.00^{aA}

Note: The data were presented as mean ± standard deviation. TSB = tryptic soy broth; Propargite = acaricide at 0.05 mg/ml; Means within the same column followed by the same lower case letters are not significantly different (p<0.05) as compared by LSD test; Means within the same row followed by the same upper case letters are not significantly different (p<0.05) as compared by LSD test.

4. Conclusion

Characterization of AgNPs and ZnNPs synthesized using *X. stockia*e PB09 cell-free supernatant has revealed some of their physical and chemical properties. The results showed that AgNPs synthesized using *X. stockia*e PB09 cell-free supernatant could form at the wavelength of 320–450 nm whereas ZnNPs synthesized using *X. stockia*e PB09 cell-free supernatant formed at the 250–450 nm, and both had their peaks at 350 nm as shown by the UV-visible spectra. Also, DLS analysis showed that the particles of AgNPs and ZnNPs synthesized using *X. stockia*e PB09 cell-free supernatant were smaller and dispersed in more organized pattern than cell-free supernatant of *X. stockia*e PB09. This may be due to the influence of adding $AgNO_3$ and $Zn(NO_3)_2$. FTIR also suggested the benefits of adding $AgNO_3$ and $Zn(NO_3)_2$ nanoparticles to cell-free supernatant of *X. stockia*e PB09 since AgNPs and ZnNPs synthesized using *X. stockia*e PB09 cell-free supernatant were found to have additional functional groups when compared to *X. stockiae* PB09 cell-free supernatant, for example, amine (1°, 2°), amide (1°, 2°), phenols, ether, bromide and chloro-iodide, all of which may play important roles on inducing the mite mortality, especially amine that could paralyze the mushroom mites (Table 1). SEM results showed that AgNPs and ZnNPs synthesized using *X. stockia*e PB09 cell-free supernatant had rougher morphology than *X. stockiae* PB09 cell-free supernatant, and they consisted of triangular and hexagonal crystals, respectively. In this study, the results showed that AgNPs and ZnNPs synthesized using *X. stockia*e PB09 cell-free supernatant could increase the efficacy of *X. stockia*e PB09 cell-free supernatant in causing mite mortality for up to 21.11% and 11.11%, respectively. AgNPs synthesized using *X. stockia*e PB09 cell-free supernatant was found to have efficacy higher than ZnNPs synthesized using *X. stockia*e PB09 cell-free supernatant for approximately 10%. In addition, the mite mortality caused by AgNPs synthesized using *X. stockia*e PB09 cell-free supernatant (93.33±3.33%) was found to be higher than that of the previous report of Bussaman *et al.* (2012) (89.00±3.60%), perhaps due to the addition of functional groups of AgNPs synthesized using *X. stockia*e PB09 as shown by FTIR analysis (Table 1). In the future, these AgNPs and ZnNPs synthesized using *X. stockia*e PB09 cell-free supernatant may be molecularly tailored to have suitable shape and size for enhancing their efficacy (Kumari *et al*., 2017). The results from this study have revealed several interesting properties of AgNPs and ZnNPs synthesized using *X. stockia*e PB09 cell-free supernatant that can be used as effective and safe biological control agents in the future.

Acknowledgements

This study was financially supported by Mahasarakham University. Thanks to the Department of Biotechnology, Faculty of Technology for providing laboratory equipment and facilities. Authors have declared no financial conflicts and any competing interests in the manuscript.

References

Abdel-Razek, A.S. 2003 Pathogenic effects of *Xenorhabdus nematophilus* and *Photorhabdus luminescens* (Enterobacteriaceae) against pupae of the Diamondback Moth, *Plutella xylostella* (L.). Journal of Pest Science. 76(4):108–111.

Ahmad, A., Wei, Y., Syed, F., Tahir, K., Rehman, A.U., Khan, A., Ullah, A., Yuan. Q. 2017. The effects of bacteria-nanoparticles interface on the antibacterial activity of green synthesized silver nanoparticles. Microbial Pathogenesis. 102:133–142.

Akhurst, R.J. 1983. Neoaplectana species: specificity of association with bacteria of the genus *Xenorhabdus*. Experimental Parasitology. 55:258–263.

Ansari, M.A., Tirry, L., Moens, M. 2003. Entomopathogenic nematodes and their symbiotic bacteria for the biological control of *Hoplia philanthus* (Coleoptera: Scarabaeidae). Biological Control. 28(1):111–117.

Barapatre, A., Ram, A. and Jha, H. 2016. Synergistic antibacterial and antibiofilm activity of silver nanoparticle biosynthesized by lignin-degrading fungus. Bioresources and Bioprocessing. 3:8.

Bharani, R.S.A. and Namasivayam, S.K.R. 2017. Biogenic silver nanoparticles mediated stress on developmental period and gut physiology of major lepidopteran pest Spodoptera litura (Fab.) (Lepidoptera: Noctuidae)—An eco-friendly approach of insect pest control. Journal of Environmental Chemical Engineering. 5:453–467.

Bode, H.B. 2009. Entomopathogenic bacteria as a source of secondary metabolite. Current Opinion in Chemical Biology. 13(2):224–230.

Bussaman, P., Sa-Uth, C., Rattanasena, P. and Chandrapatya, A. 2012. Acaricidal activities of whole cell suspension, cell-free supernatant, and crude cell extract *of Xenorhabdus stockiae* against mushroom mite (*Luciaphorus* sp.). Journal of Zhejing University Science B. 13(4):261–266.

Bussaman, P., Sobanboa, S., Grewal, P.S. and Chandrapatya, A. 2009. Pathogenicity of additional strains of Photorhabdus and Xenorhabdus (Enterobacteriaceae) to the mushroom mite *Luciaphorus perniciosus* (Acari : Pygmephoridae). Applied Entomology and Zoology. 44(2):293–299.

Fang, X.L., Zhang, M., Tang, Q., Wang, Y., and Zhang, X. 2014. Inhibitory effect of *Xenorhabdus nematophila* TB on plant pathogens *Phytophthora capsici* and *Botrytis cinerea* in vitro and in planta. Scientific Reports. 4:4300.

Forst, S., Dowds, B., Boemare, N. and Stackebrandt, E. 1997. *Xenorhabdus* and *Photorhabdus* spp.: bugs the kill bugs. Annual Review of Microbiology. 51(1):47–72.

Forst, S., and Nealson, K. 1996. Molecular biology of the symbiotic-pathogenic bacteria *Xenorhabdus* spp. and *Photorhabdus* spp. Microbiological Reviews. 60(1):21–43.

Gandhi, P.R., Jayaseelan, C., Mary, R.R., Mathivanan, D. and Suseem, S.R. 2017. Acaricidal, pediculicidal and larvicidal activity of synthesized ZnO nanoparticles using Momordica charantia leaf extract against blood feeding parasites. Experimental Parasitology. 181:47–56.

Ghiuta, I., Cristea, D. Croitoru, C. Kost, J. Wenkert, R. Vyrides, I. Anayiotos, A. and Munteanu, D. 2017. Characterization and antimicrobial activity of silver nanoparticles, biosynthesized using Bacillus species. Applied Surface Science. 438:66–73.

Kumari, M., Pandey, S., Giri, V.P., Bhattacharya, A., Shukla, R., Mishra, A. and Nautiyal C.S. 2017. Tailoring shape and size of biogenic silver nanoparticles to enhance antimicrobial efficacy against MDR bacteria. Microbial Pathogenesis. 105:346–355.

Mahar, A.N., Munir, M., Elawad, S., Gowen, S.R., Hague, N.G.M. 2005. Pathogenicity of bacterium, *Xenorhabdus nematophila* isolated from entomopathogenic nematode (*Steinernema carpocapsae*) and its secretion against *Galleria mellonella* larvae. Journal of Zhejiang University Science B. 6(6):457–463.

Nielsen-LeRoux, C., Gaudriault, S., Ramarao, N., Lereclus, D., and Givaudan, A. 2012. How the insect pathogen bacteria *Bacillus thuringiensis* and *Xenorhabdus / Photorhabdus* occupy their hosts. Current Opinion in Microbiology. 15(3):220–231.

Patra, J.K. and Baek, K.H. 2017. Antibacterial activity and synergistic antibacterial potential of biosynthesized silver nanoparticles against foodborne pathogenic bacteria along with its anticandidal and antioxidant effects. Frontiers in Microbiology. 8:1–14.

Sardella, D., Gatt, R. and Valdramidis, V.P. 2017. Physiological effects and mode of action of ZnO nanoparticles against postharvest fungal contaminants. Food Research International. 101:274–279.